COMMUNICATIONS PHYSICS

ARTICLE

https://doi.org/10.1038/s42005-020-0283-9 OPEN

Ultrafast photonics of two dimensional $AuTe_2Se_{4/3}$ in fiber lasers

Wenjun Liu [1,2], Mengli Liu[1,2], Xu Chen[2], Tao Shen[3], Ming Lei[1]*, Jiangang Guo[2], Huixiong Deng[3], Wei Zhang [4], Chaoqing Dai[5]*, Xiaofei Zhang[6] & Zhiyi Wei[2]*

The exploration of promising nonlinear optical materials, which allows for the construction of high-performance optical devices in fundamental and industrial applications, has become one of the fastest-evolving research interests in recent decades and plays a key role in the development and innovation of optics in the future. Here, by utilizing the optical nonlinearity of a recently synthesized, two dimensional material $AuTe_2Se_{4/3}$ prepared by the self-flux method, a passively mode-locked fiber laser operating at 1557.53 nm is achieved with 147.7 fs pulse duration as well as impressive stability (up to 91 dB). The proposed mode-locked fiber laser reveals superior overall performance compared with previously reported lasers which are more widely studied in the same band. Our work not only investigates the optical nonlinearity of $AuTe_2Se_{4/3}$, but also demonstrates its ultrafast photonics application. These results may stimulate further innovation and advancement in the field of nonlinear optics and ultrafast photonics.

[1] State Key Laboratory of Information Photonics and Optical Communications, School of Science, Beijing University of Posts and Telecommunications, P. O. Box 122, Beijing 100876, China. [2] Beijing National Laboratory for Condensed Matter Physics, Institute of Physics, Chinese Academy of Sciences, Beijing 100190, China. [3] State Key Laboratory of Superlattices and Microstructures, Institute of Semiconductors, Chinese Academy of Sciences & Center of Materials Science and Optoelectronics Engineering, University of Chinese Academy of Sciences, Beijing 100083, China. [4] Chongqing Institute of Green and Intelligent Technology, Chinese Academy of Sciences, Chongqing 400714, China. [5] Zhejiang A&F University, School of Science, Lin'an, Zhejiang 311300, China. [6] Key Laboratory of Time and Frequency Primary Standards, National Time Service Center, Chinese Academy of Sciences, Xi'an 710600, China. *email: mlei@bupt.edu.cn; dcq424@126.com; zywei@iphy.ac.cn

Nonlinear optics, as an important discipline describing the interaction between light and material, has become one of the fastest-evolving scientific fields in recent decades[1]. In this discipline, the nonlinear response of materials to external electromagnetic field under linear field amplitude has been studied in depth. Optical nonlinearity is also the intrinsic cause of some interesting optical phenomena, such as optical rectification, Kerr effect, higher harmonics and saturable absorption[2–5]. It is believed that the explorations of promising nonlinear optical materials for fundamental and industrial applications play a key role in the development and innovation of optics in the future.

In recent years, femtosecond lasers, which are widely applied in micromachining[6], medical operation[7,8], molecular spectroscopy[9,10], and optical communications[11], have become good platforms for nonlinear materials to be applied effectively. After the early use of semiconductor saturable absorber mirrors, the nonlinear proof and experimental observation of graphene have aroused the upsurge of research on two dimensional (2D) materials[12–16]. Subsequently, black phosphorus[17–19], topological insulators[20–22] and transition metal dichalcogenides[23–25] have been extensively studied. The high third-order optical nonlinearity, simplicity of fabrication and ultrafast excited state carrier dynamics of mentioned 2D materials have endowed them unique advantages in laser applications. Meanwhile, the research and attempt on new materials are still going on[26–28].

Recently, a new 2D material $AuTe_2Se_{4/3}$ has been successfully prepared by Guo et al.[29]. Through the introduction of Se element, they have successfully transformed the three-dimensional disordered cubic $AuTe_2$ phase into a 2D layered structure, and have proved that the 2D state of $AuTe_2Se_{4/3}$ comes from the Berezinsky-Kosterlitz-Thouless topological transition. As the main nonlinear source of optical modulators, 2D materials have a huge impact on the performance of lasers. Thus, $AuTe_2Se_{4/3}$ may bring about new breakthroughs and opportunities in ultrafast photonics. However, the potential applications of $AuTe_2Se_{4/3}$ in ultrafast photonics have not been explored yet.

In this paper, the possibility of generating mode-locked pulses by $AuTe_2Se_{4/3}$ is investigated by a combination of experiments and calculations, in which $AuTe_2Se_{4/3}$ is used as a saturable absorber (SA). By utilizing the optical nonlinearity of $AuTe_2Se_{4/3}$ prepared by the self-flux method, a passively mode-locked fiber laser operating at 1557.53 nm has been demonstrated, which features ultrafast pulse duration (147.7 fs) as well as impressive stability (up to 91 dB). From the comparison with previously reported lasers which are more widely studied in the same band, the overall performance of the proposed lasers is highlighted. Experimental results suggest that $AuTe_2Se_{4/3}$ is a kind of excellent nonlinear optical materials, and has advantages in ultrafast photonics application.

Results

Preparation and characterization. The band structure and total energy calculations of $AuTe_2Se_{4/3}$ are presented in Supplementary Note 1, which indicates the $AuTe_2Se_{4/3}$ is a metallic material with environmental stability. The process of preparation and transfer of $AuTe_2Se_{4/3}$ is described in Fig. 1. The detailed operation process is discussed in "Methods" section. Figure 2a shows powder x-ray diffraction pattern of $AuTe_2Se_{4/3}$ single crystal. Only (00 l) Bragg peaks show up, suggesting that the crystallographic *c*-axis is perpendicular to the plane of the single crystal. The peaks are sharp and well-defined, indicating good crystallized quality. A transmission electron microscope (TEM) image of exfoliated thin flake of $AuTe_2Se_{4/3}$ shows a good 2D layer of *ab* plane in Fig. 2b. Besides, Fig. 2c displays the high resolution TEM (HRTEM) image, and the corresponding selected-area electron diffraction (SAED) pattern is presented. The atomic intra-spacing of two perpendicular direct is about 2.8 Å, which corresponds to the interlayer spacing of (310) or (031) plane[29]. The chemical composition is further investigated by x-ray photoelectron spectroscopy (XPS). The Te peaks ($3d_{5/2}$ at 573.30 eV, $3d_{3/2}$ at 483.74 eV), Au peaks ($3f_{7/2}$ at 84.37 eV, $3f_{5/2}$ at 88.03 eV) and Se peaks ($2d_{5/2}$ at 53.59 eV, $2d_{3/2}$ at 54.31 eV) can be observed in Fig. 2d. The atomic force microscopy (AFM) image of ultrasonically exfoliated thin-flake with the 5 nm thickness, which equates to the 5 layers of $AuTe_2Se_{4/3}$, is shown in Fig. 2e.

By using the balanced twin-detector measurement system, the saturable absorption property of the $AuTe_2Se_{4/3}$ SA is investigated. The schematic diagram of the balanced twin-detector measurement system is shown in Fig. 3a. The incident optical pulses come from a home-made mode-locked laser with the pulse duration of 700 fs and repetition rate of 120 MHz. The source light from the mode-locked laser is divided into two parts by a 50:50 output coupler (OC). It is worth noting that by adjusting the variable optical attenuator (VOA) before OC, the power of light passing through OC in the total channel can be changed. Half of the light divided by OC is measured directly by the detector of the power meter for reference. The other half is received by the detector after the saturable absorption of the $AuTe_2Se_{4/3}$ SA. Saturable absorption at a given power can be obtained by the ratio of two power channels. With the adjustment of VOA, the whole process of the SA from light absorption to light saturation in wide power range can be obtained, as shown in Fig. 3b. From the fitted absorption curves, the modulation depth of the $AuTe_2Se_{4/3}$ SA is about 65.58%.

Mode-locked fiber laser. The experimental schematic design of the proposed laser, which is used to prove the optical nonlinearity of the $AuTe_2Se_{4/3}$ SA, is shown in Fig. 4. The erbium-doped fiber (EDF) laser is formed by the 0.6 m-long EDF (Liekki 110-4/125), a 20:80 OC, an isolator (ISO) and a polarization controller (PC). The main function of the PC is to adjust the polarization state and optimize the laser state. The $AuTe_2Se_{4/3}$ SA is successively placed between ISO and PC. The standard SMF-28 fibers are commonly used to make up the pigtails of all optical elements. The whole system is pumped by a commercial stabilized laser diode (LD), which operates at 980 nm and owns the maximum

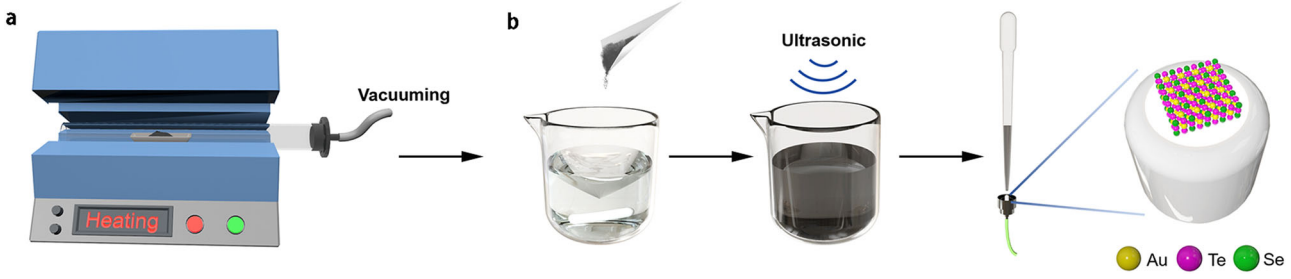

Fig. 1 Schematic preparation process of the $AuTe_2Se_{4/3}$ saturable absorber (SA). a the self-flux method. **b** the transfer process of $AuTe_2Se_{4/3}$.

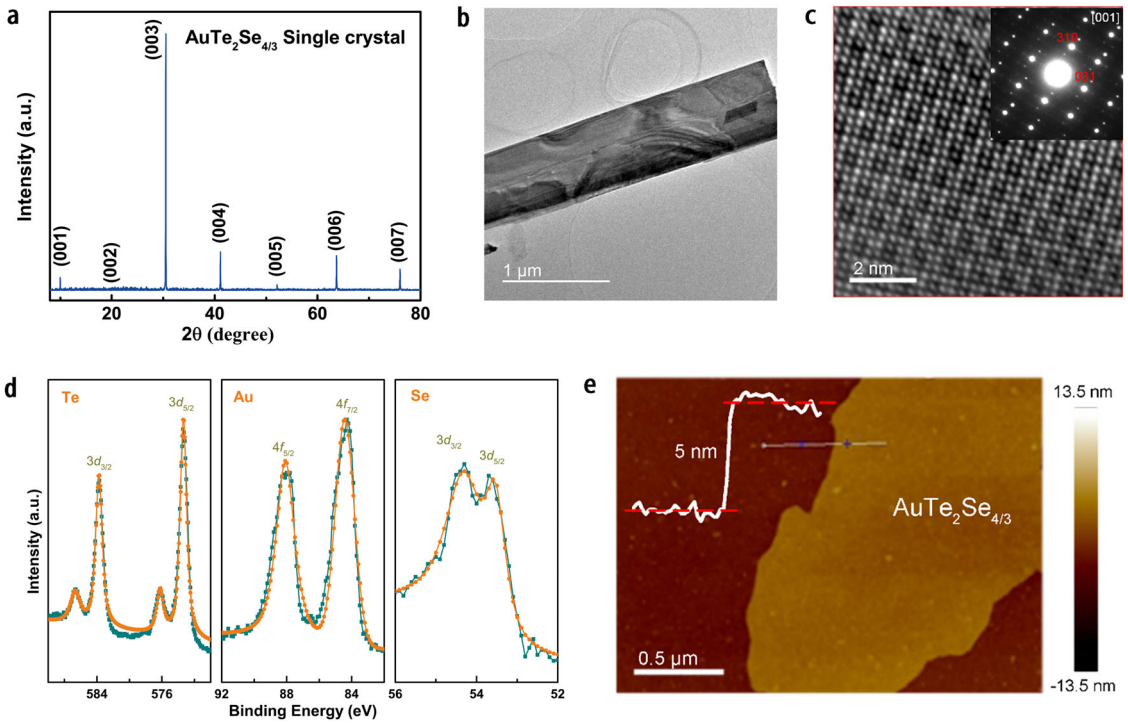

Fig. 2 The characterization of $AuTe_2Se_{4/3}$. **a** X-ray diffraction (XRD) pattern. **b** Transmission electron microscope (TEM) images. **c** High resolution TEM (HR-TEM) and selected-area electron diffraction (SAED) (inset) images. **d** x-ray photoelectron spectroscopy (XPS) of Te 3*d*, Au 4*f* and Se 3*d* of the $AuTe_2Se_{4/3}$ crystal. **e** Atomic force microscopy (AFM) images of $AuTe_2Se_{4/3}$ saturable absorber (SA) and typical height profiles.

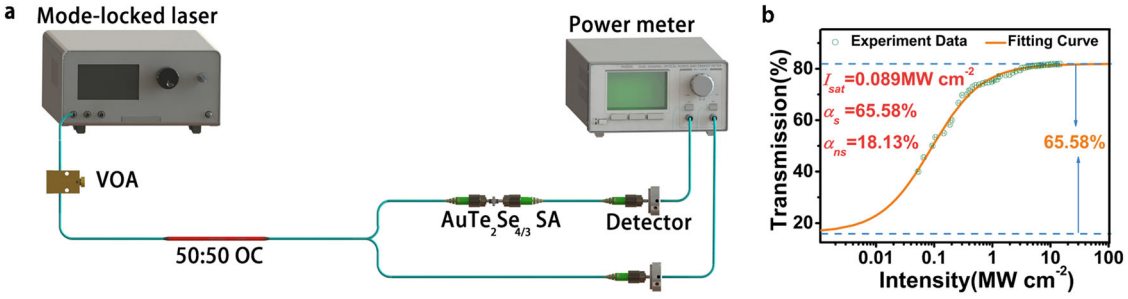

Fig. 3 Nonlinear measurement of $AuTe_2Se_{4/3}$ saturable absorber (SA). **a** Schematic diagram of saturable absorption measurement. VOA: variable optical attenuators; OC: optical coupler. **b** Nonlinear transmission of the $AuTe_2Se_{4/3}$ saturable absorber (SA). The error of the power is ± 5% due to the uncertainty of the power monitors.

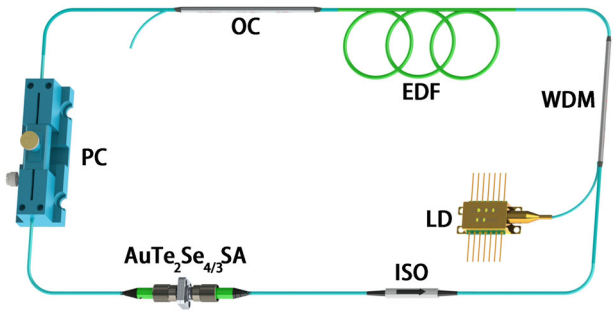

Fig. 4 The experimental schematic design of the proposed laser. LD: laser diode; WDM: wavelength division multiplexor; EDF: erbium-doped fiber; OC: output coupler; PC: polarization controller; ISO: isolator.

output power of 630 mW. The wavelength division multiplexor (WDM) is the key interface unit for guiding pumped light into the cavity. With 20% of the light output from the cavity, the working status of the laser can be observed on the oscilloscope (Tektronix DPO3054) in time. The corresponding spectra and radio frequency (RF) spectrum can be measured with the help of spectrum analyzer (Yokogawa AQ6370C) and RF spectrum analyzer (Agilent E4402B).

With the coordination of the gradual increase of pump power and proper adjustment of PC, the mode-locked pulses are generated. At the pump power of 93 mW, the stable mode-locked pulses are successfully observed on oscilloscope. The round-trip time of pulses shown in Fig. 5a conforms to the fundamental frequency of 69.9 MHz. From the optical spectrum in Fig. 5b, the center wavelength of the mode-locked pulse is 1557.53 nm with the 3-dB bandwidth of 30.26 nm. As shown in Fig. 5c, the

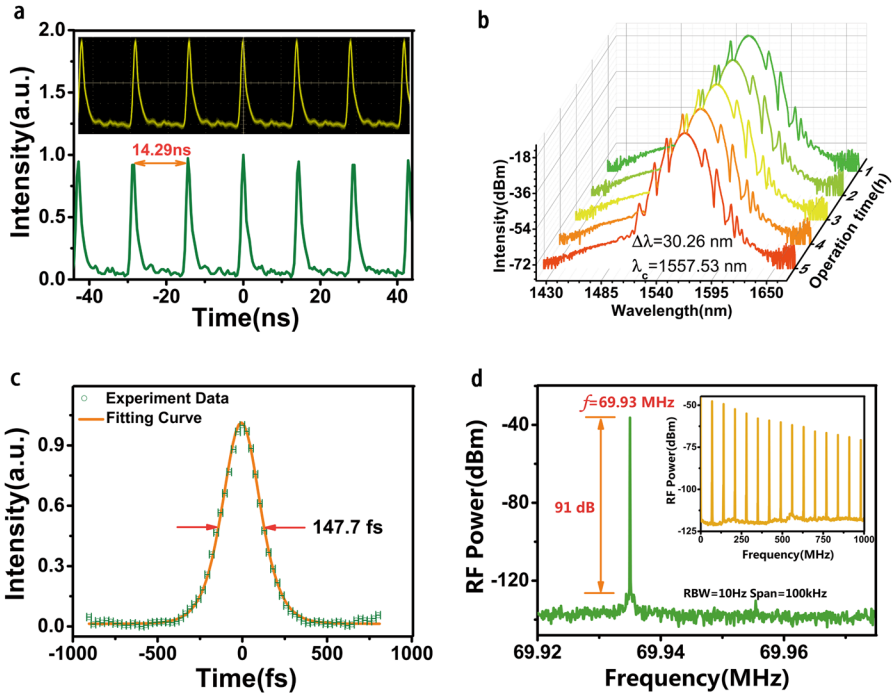

Fig. 5 The Er-doped fiber laser performance mode-locked by the $AuTe_2Se_{4/3}$ saturable absorber (SA). a Stable mode-locked pulse train. **b** Long-term monitoring for mode-locked spectrum. **c** Autocorrelation traces of mode-locked pulses. The error of the pulse duration is ±7 fs due to the uncertainty of the autocorrelation instrument. **d** Radio frequency (RF) spectrum of mode-locked pulses with resolution bandwidth of 10 Hz (the illustrations is the RF spectrum with the wide band of 1 GHz).

pulse duration of the mode-locked pulse is as short as 147.7 fs after the sech[2] fitting. Further, the time-bandwidth product of the system is calculated as 0.5523. The RF spectrum of the pulse is shown in Fig. 5d. The signal-to-noise ratio (SNR) of the fundamental repetition rate is measured as 91 dB. Moreover, no significant interference peaks are observed in the illustrations in Fig. 5d with the wide band of 1 GHz. In other words, the mode-locked system works well with good stability. The output power of the proposed mode-locked laser versus pump power are provided in Fig. 6. The average output power of the proposed laser is 21.4 mW. When the $AuTe_2Se_{4/3}$ SA is removed, the mode-locked pulses could not be obtained at the same cavity. This result indicates that the optical nonlinearity of the $AuTe_2Se_{4/3}$ SA is the main cause of the mode-locking phenomenon. The optical damage threshold of $AuTe_2Se_{4/3}$ SA is about 0.169 J cm^{-2}.

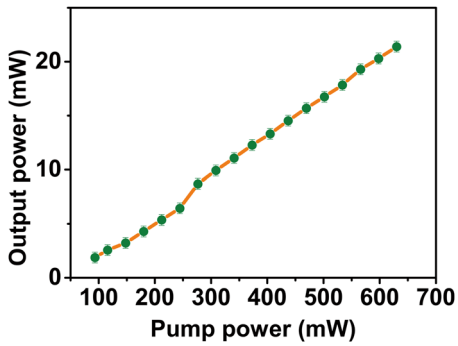

Fig. 6 The output power of the proposed mode-locked laser varies with the pump power. The error of the power is ±5% due to the uncertainty of the power monitors.

Discussion

The overall performance of the proposed laser based on the $AuTe_2Se_{4/3}$ SA and previously reported lasers which are more widely studied in the same band are summarized in Table 1. Modulation depth, as an important parameter reflecting the regulation ability of materials for light, has an important reference role in evaluating SA ability. It has reported that materials with large modulation depth are conducive to the formation of ultrashort pulses[39]. In Table 1, the modulation depth of $AuTe_2Se_{4/3}$ SA is up to 65.58%, which is the largest. The output power of 21. 4 mW is the highest. The SNR up to 91 dB reveals the stability of the whole mode-locked system, which is proved to be superior by comparison. In terms of the pulse duration, the proposed laser is only inferior to that of the carbon nanotube (CNT). However, considering that the absorption wavelength of the CNT is related to its diameter, it is necessary to select CNTs with different diameters in different wavelength bands. This property is not conducive to broadband applications. $AuTe_2Se_{4/3}$ is considered to be a metallic material after the theoretical calculation, which indicates that it has great potential in broadband absorption application. Therefore, in terms of broadband absorption characteristics and overall performance, $AuTe_2Se_{4/3}$ can be a strong candidate for a new generation of SAs.

In summary, the 2D material $AuTe_2Se_{4/3}$ has shown good prospects for saturable absorption applications in theory and experiment. The DFT calculations of $AuTe_2Se_{4/3}$ indicates that it is a metallic material with environmental stability. Based on the $AuTe_2Se_{4/3}$ SA, the mode-locked pulses have been realized in the fiber laser based on the nonlinear optical properties of $AuTe_2Se_{4/3}$. Besides, compared with previously reported lasers which are widely studied in the same band, the 147.7 fs pulse duration and 91 dB SNR of the proposed laser are the best. Moreover, the proposed $AuTe_2Se_{4/3}$ has better results in overall performance, especially in the ultrafast photonics application. This potential in ultrafast optics may stimulate further innovation and progress in related nonlinear optics and photonic applications.

Table 1 Comparison between mode-locked lasers based on different SAs.

Materials	MD (%)	Δλ/λ (nm)	τ (fs)	P (mW)	SNR (dB)	Refs.
Graphene	3.6	6/1555	590	0.91	70	30
CNT	15.8	41/1554	97	3.93	-	31
BPs	8.1	2.9/1571.45	946	-	70	32
Sb_2Te_3	3.9	6/1556	449	0.9	74	33
Bi_2Se_3	3.9	4.3/1557.5	660	1.8	55	34
WS_2	2.9	5.2/1572	595	~7	75	35
MoS_2	4.3	4/1569.5	710	1.78	60	36
$MoSe_2$	0.63	1.76/1558.25	1450	0.44	61.5	37
WSe_2	0.3	2/1556.7	1310	0.45	~50	38
$AuTe_2Se_{4/3}$	65.58	30.26/1557.53	147.7	21.4	91	This work

Methods

Sample fabrication. By the self-flux method, $AuTe_2Se_{4/3}$ was successfully grown as shown in Fig. 1a. The detailed operation process is as follows. At first, three high-quality powders including Se powder (99.99%, Sigma Aldrich), Te powder (99.999%, Sigma Aldrich) and Au powder (99.99%, Sigma Aldrich) were prepared. After the stoichiometric weighting, the starting materials with a weight of 2–4 g were sealed in the evacuated silica tube with a vacuum of 10^{-5} mbar. Then, the sealed materials were loaded into the muffle furnace. When the materials were ready, the temperature in the furnace was increased to 800 °C and remained for 10 h. After that, the temperature in the furnace was dropped to 450 °C uniformly within 4 days, and then the furnace was turned off. As shown in Fig. 1b, 60 mg of $AuTe_2Se_{4/3}$ was added to 20 mL of ethanol and treated with ultrasonic for 20 min until it was completely dispersed in ethanol. Subsequently, 40 μL of the dispersion was dropped on the end face of fiber. After drying at room temperature, the $AuTe_2Se_{4/3}$ SA was fabricated.

Data availability

The data that support the findings of this study are available from the corresponding authors upon reasonable request. The DOI of the data is https://doi.org/10.6084/m9.figshare.11363099.v4.

Received: 5 July 2019; Accepted: 23 December 2019;
Published online: 21 January 2020

References

1. Boyd, R. W. in Nonlinear Optics, 3rd edn., (Academic Press, Cambridge, MA, USA, 2008).
2. Franken, P. A., Hill, A. E., Peters, C. W. & Weinreich, G. Generation of optical harmonics. *Phys. Rev. Lett.* **7**, 118 (1961).
3. Kerr, J. L. A new relation between electricity and light: Dielectrified media birefringent. *Philos. Mag.* **50**, 337–348 (1875).
4. Bass, M., Franken, P. A., Ward, J. F. & Weinreich, G. Optical rectification. *Phys. Rev. Lett.* **9**, 446 (1962).
5. Colin, S., Contesse, E., Le Boudec, P., Stephan, G. & Sanchez, F. Evidence of a saturable-absorption effect in heavily erbium-doped fibers. *Opt. Lett.* **21**, 1987–1989 (1996).
6. Gattass, R. R. & Mazur, E. Femtosecond laser micromachining in transparent materials. *Nat. Photon.* **2**, 219–225 (2008).
7. Merker, M., Ackermann, R., Kammel, R. & Kunert, K. S. An in vitro study on focusing fs-laser pulses into ocular media for ophthalmic surgery. *Laser Surg. Med.* **45**, 589–596 (2013).
8. Morin, F., Druon, F., Hanna, M. & Georges, P. Microjoule femtosecond fiber laser at 1.6 μm for corneal surgery applications. *Opt. Lett.* **34**, 1991–1993 (2009).
9. Diddams, S. A., Hollberg, L. & Mbele, V. Molecular fingerprinting with the resolved modes of a femtosecond laser frequency comb. *Nature* **445**, 627–630 (2007).
10. Xu, C. & Wise, F. W. Recent advances in fibre lasers for nonlinear microscopy. *Nat. Photon.* **7**, 875–882 (2013).
11. De Vivie-Riedle, R. & Troppmann, U. Femtosecond lasers for quantum information technology. *Chem. Rev.* **107**, 5082–5100 (2007).
12. Liverini, V. et al. Low-loss GaInNAs saturable absorber mode locking a 1.3-μm solid-state laser. *Appl. Phys. Lett.* **84**, 4002–4004 (2004).
13. Keller, U. Recent developments in compact ultrafast lasers. *Nature* **424**, 831–838 (2003).
14. Novoselov, K. S. et al. Electric field effect in atomically thin carbon films. *Science* **306**, 666–669 (2004).
15. Bao, Q. et al. Atomic-layer graphene as a saturable absorber for ultrafast pulsed lasers. *Adv. Funct. Mater.* **19**, 3077–3083 (2009).
16. Sun, Z. et al. Graphene mode-locked ultrafast laser. *ACS Nano* **4**, 803–810 (2010).
17. Na, D. et al. Passivation of black phosphorus saturable absorbers for reliable pulse formation of fiber lasers. *Nanotechnology* **28**, 475207 (2017).
18. Rodin, A. S., Carvalho, A. & Neto, A. H. C. Strain-induced gap modification in black phosphorus. *Phys. Rev. Lett.* **112**, 176801 (2014).
19. Han, C. Q. et al. Electronic structure of black phosphorus studied by angle-resolved photoemission spectroscopy. *Phys. Rev. B.* **90**, 085101 (2014).
20. Yan, P., Lin, R., Ruan, S., Liu, A. J. & Chen, H. A 2.95 GHz, femtosecond passive harmonic mode-locked fiber laser based on evanescent field interaction with topological insulator film. *Opt. Express* **23**, 154–164 (2015).
21. Lin, Y. H. et al. Soliton compression of the erbium-doped fiber laser weakly started mode-locking by nanoscale p-type Bi_2Te_3 topological insulator particles. *Laser Phys. Lett.* **11**, 055107 (2014).
22. Zhang, H. et al. Topological insulators in Bi_2Se_3, Bi_2Te_3 and Sb_2Te_3 with a single Dirac cone on the surface. *Nat. Phys.* **5**, 438–442 (2009).
23. Sotor, J. et al. Mode-locking in Er-doped fiber laser based on mechanically exfoliated Sb_2Te_3 saturable absorber. *Opt. Mater. Express* **4**, 1–6 (2014).
24. Zhao, C. et al. Ultra-short pulse generation by a topological insulator based saturable absorber. *Appl. Phys. Lett.* **101**, 211106 (2012).
25. Luo, Z. et al. 1-, 1.5-, and 2-μm fiber lasers Q-switched by a broadband few-layer MoS_2 saturable absorber. *J. Lightwave Technol.* **32**, 4077–4084 (2014).
26. Xu, Y. et al. Solvothermal synthesis and ultrafast photonics of black phosphorus quantum dots. *Adv. Opt. Mater.* **4**, 1223–1229 (2016).
27. Jiang, X. et al. Broadband nonlinear photonics in few-layer MXene $Ti_3C_2T_x$ (T = F, O, or OH). *Laser Photonics Rev.* **12**, 1700229 (2018).
28. Yang, L. et al. Gold nanostars as a Q-switcher for the mid-infrared erbium-doped fluoride fiber laser. *Opt. Lett.* **21**, 5459–5462 (2018).
29. Guo, J. G. et al. Quasi-two-dimensional superconductivity from dimerization of atomically ordered $AuTe_2Se_{4/3}$ cubes. *Nat. Commun.* **8**, 871 (2017).
30. Sobon, G., Sotor, J. & Abramski, K. M. All-polarization maintaining femtosecond Er-doped fiber laser mode-locked by graphene saturable absorber. *Laser Phys. Lett.* **9**, 581 (2012).
31. Wang, J. et al. Pulse dynamics in carbon nanotube mode-locked fiber lasers near zero cavity dispersion. *Opt. Express* **23**, 9947–9958 (2015).
32. Chen, Y. et al. Mechanically exfoliated black phosphorus as a new saturable absorber for both Q-switching and mode-locking laser operation. *Opt. Express* **23**, 12823–12833 (2015).
33. Boguslawski, J. et al. Mode-locked Er-doped fiber laser based on liquid phase exfoliated Sb_2Te_3 topological insulator. *Laser Phys.* **24**, 105111 (2014).
34. Liu, H. et al. Femtosecond pulse generation from a topological insulator mode-locked fiber laser. *Opt. Express* **6**, 6868–6873 (2014).
35. Wu, K., Zhang, X. Y., Wang, J., Li, X. & Chen, J. P. WS_2 as a saturable absorber for ultrafast photonic applications of mode-locked and Q-switched lasers. *Opt. Express* **23**, 11453–11461 (2015).
36. Liu, H. et al. Femtosecond pulse erbium-doped fiber laser by a few-layer MoS_2 saturable absorber. *Opt. Lett.* **39**, 4591–4594 (2014).
37. Luo, Z. et al. Nonlinear optical absorption of few-layer molybdenum diselenide ($MoSe_2$) for passively mode-locked soliton fiber laser. *Photonics Res.* **3**, A79–A86 (2015).
38. Mao, D. et al. Erbium-doped fiber laser passively mode locked with few-layer $WSe_2/MoSe_2$ nanosheets. *Sci. Rep.* **6**, 23583 (2016).
39. Jeon, J., Lee, J. & Lee, J. H. Numerical study on the minimum modulation depth of a saturable absorber for stable fiber laser mode locking. *J. Opt. Soc. Am. B.* **32**, 31–37 (2015).

Acknowledgements

We acknowledge the financial support from the National Natural Science Foundation of China (NSFC) (11674036; 11875008; 91850209); Beijing Youth Top-Notch Talent Support Program (2017000026833ZK08); Fund of State Key Laboratory of Information Photonics

and Optical Communications (Beijing University of Posts and Telecommunications, IPOC2019ZZ01); The Fundamental Research Funds for the Central Universities (500419305); State Key Laboratory of Advanced Optical Communication Systems and Networks, Shanghai Jiao Tong University (2019GZKF03007); Beijing University of Posts and Telecommunications Excellent Ph.D. Students Foundation (CX2019202).

Author contributions

W.L., M.Liu, X.C., and J.G. fabricated the samples. W.L., M.Liu, X.C., M.Lei and J.G. performed the measurements. X.C., M.Lei, and J.G. performed the TEM results. W.L., T.S., H.D., W.Z., C.D., and X.Z. developed the theory. W.L. and Z.W. designed the project. All authors discussed the result, and contributed to the writing of the manuscript.

Competing interests

The authors declare no competing interests.

Additional information

Supplementary information is available for this paper at https://doi.org/10.1038/s42005-020-0283-9.

Correspondence and requests for materials should be addressed to M.L., C.D. or Z.W.

Reprints and permission information is available at http://www.nature.com/reprints

Publisher's note Springer Nature remains neutral with regard to jurisdictional claims in published maps and institutional affiliations.